Hydrothermal breakdown of chevkinite-(Ce)

- evidence from experiments

Daniel HARLOV

Bogusław BAGIŃSKI
Ray MACDONALD
Petras JOKUBAUSKAS
Witold MATYSZCZAK

Reactions occuring at mineral-fluid boundries are important for the cycling of elements in different environments.

The common feature is that a mineral assemblage in a contact with fluid may be replaced by a more stable one.

Understanding the transformation mechanisms of one solid phase to another and role of fluids is fundamental to many natural processes.

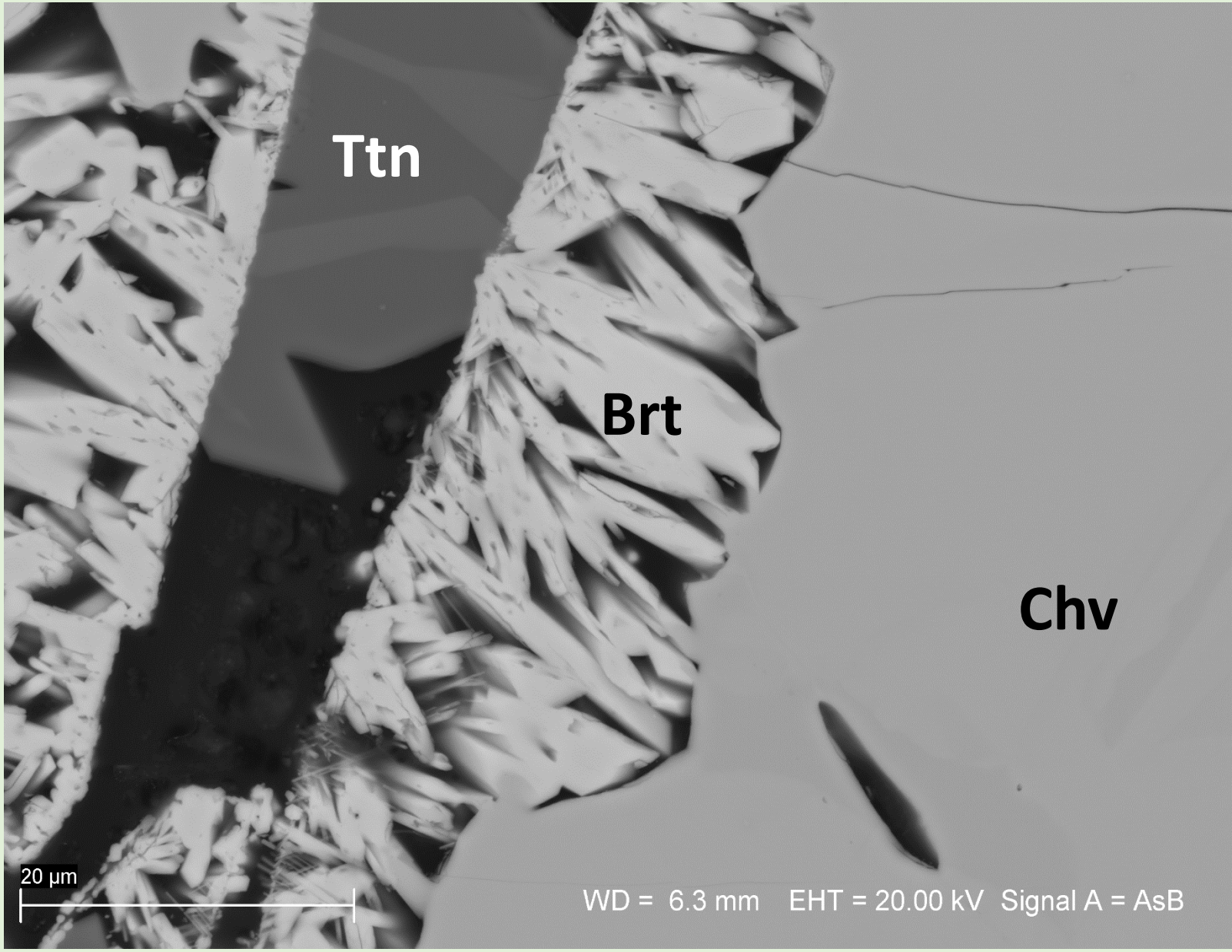

“Standard” formula of chevkinite-group of minerals

$$A_4BC_2D_2(Si_2O_7)_2O_8$$

where

A = REE, Ca, Sr

B = Fe^{2+}

C = Fe^{2+}, Fe^{3+}, Ti, Al

D = Ti

But **56** elements recorded at ppm to percent level (16 at % level)

Members of the chevkinite group,

(accepted by the CNMNC-IMA)

Mineral	Formula	Reference
Chevkinite subgroup		
Chevkinite-(Ce)	$(REE,Ca)_4Fe^{2+}(Ti,Fe^{3+},Fe^{2+},Al)_2Ti_2Si_4O_{22}$	Ito, Arem (1971)
Polyakovite-(Ce)	$(REE,Ca)_4(Mg,Fe^{2+})(Cr,Fe^{3+})_2(Ti,Nb)_2Si_4O_{22}$	Sokolova et al. (2001)
Maoniupingite-(Ce)	$(REE,Ca)_4(Fe^{3+},Ti,Fe^{2+},\square)(Fe^{3+},Fe^{2+},Nb,Ti)_2Ti_2Si_4O_2$	Shen et al. (2005)
Dingdaohengite-(Ce)	$Ce_4Fe^{2+}Ti_2Ti_2(Si_2O_7)_2O_8$	Xu et al. (2008)
Christofschäferite-(Ce)	$(Ce,La,Ca)_4Mn(Ti,Fe^{3+})_3(Fe^{3+},Fe^{2+},Ti)(Si_2O_7)_2O_8$	Chukanov et al. (2012)
Delhuyarite-(Ce)	$Ce_4Mg(Fe^{3+}{}_2W)\square(Si_2O_7)_2O_6(OH)_2$	Holstam et al. (2017)
Perrierite subgroup		
Perrierite-(Ce)	$(REE,Ca)_4Fe^{2+}(Ti,Fe^{3+},Fe^{2+},Al)_2Ti_2Si_4O_{22}$	Ito, Arem (1971)
Strontiochevkinite	$(Sr_2[La,Ce]_{1.5}Ca_{0.5})_4Fe^{2+}{}_{0.5}Fe^{3+}{}_{0.5}(Ti,Zr)_4Si_4O_{22}$	Haggerty, Mariano (1983)
Rengeite	$Sr_4ZrTi_4Si_4O_{22}$	Miyajima et al. (2001)
Matsubaraite	$Sr_4Ti_5(Si_2O_7)_2O_8$	Miyajima et al. (2002)
Hezuolinite	$(Sr,REE)_4Zr(Ti,Fe^{3+},Fe^{2+})_2Ti_2O_8(Si_2O_7)_2$	Yang et al. (2012)
Perrierite-(La)	$(La,Ce,Ca)_4(Fe^{2+},Mn)(Ti,Fe^{3+},Al)_4(Si_2O_7)_2O_8$	Chukanov et al. (2011)

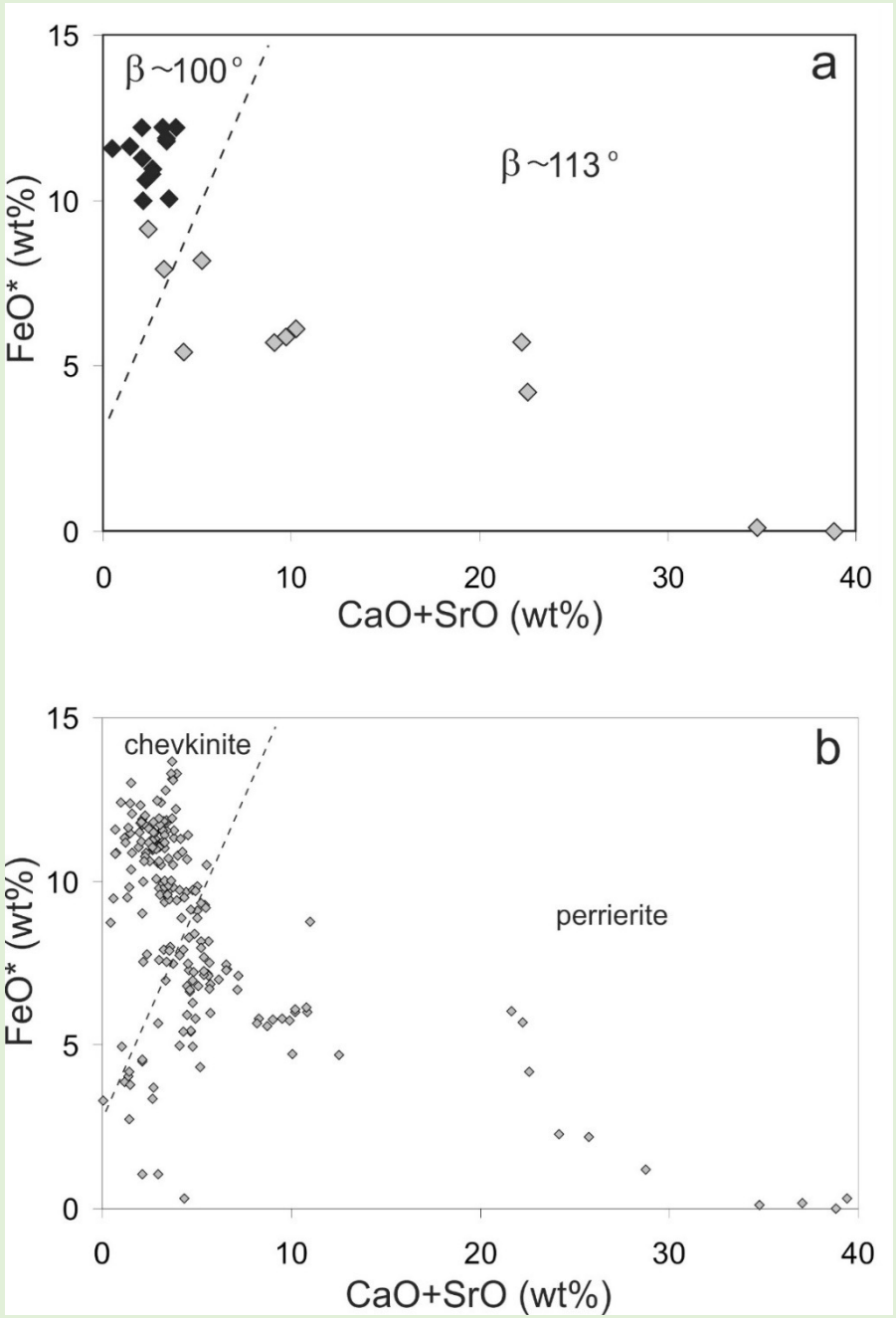

How we distinguish chevkinite from perrierite

The (CaO+SrO) – FeO* (all Fe as Fe2+) plot used as an empirical discriminant between the chevkinite and perrierite subgroups by Macdonald and Belkin (2002) and modified by Macdonald et al. (2009). Data plotted are for crystals that have had the b angle determined, updated with post-2009 data.

Chevkinite group of minerals : conditions of formation

Pressure	≥50 to ≤1 kbar
Temperature	~1200 to 350°C (both rather poorly constrained)
$f\mathbf{O}_2$	ΔFMQ -2 to +5
$p\mathbf{H_2O}$	from “dry” (high-grade metam) to water-saturated (exptal)

Experimental work has been carried out in the GeoForschungsZentrum Potsdam Hydrothermal laboratory

GFZ Helmholtz-Zentrum POTSDAM

Equipment

Two Johannes-type piston cylinders: 400-1000°C; 500-2000 MPa.

One end load piston cylinder: 600-1200°C; 800-4000 Mpa

Hydrothermal line – cold seal autoclaves: 300-750°C; 100-500 MPa.

Noble metal tubing; laboratory facilities for the loading and sealing of noble metal capsules. Max. thermal gradient along the length of capsule is approx. 5°C. Accurancy of temp. ±3°C

Experiment

Chevkinite-(Ce) (Diamer District, Pakistan)	15 mg
Quartz	5 mg
Albite	5 mg
$Ca(OH)_2$	1 mg
H_2O	5 mg

desired T (˚C)	600 ˚C
desired P (MPa/kbar)	400/4
total run time	21 days

Picture of the sample after the experiment

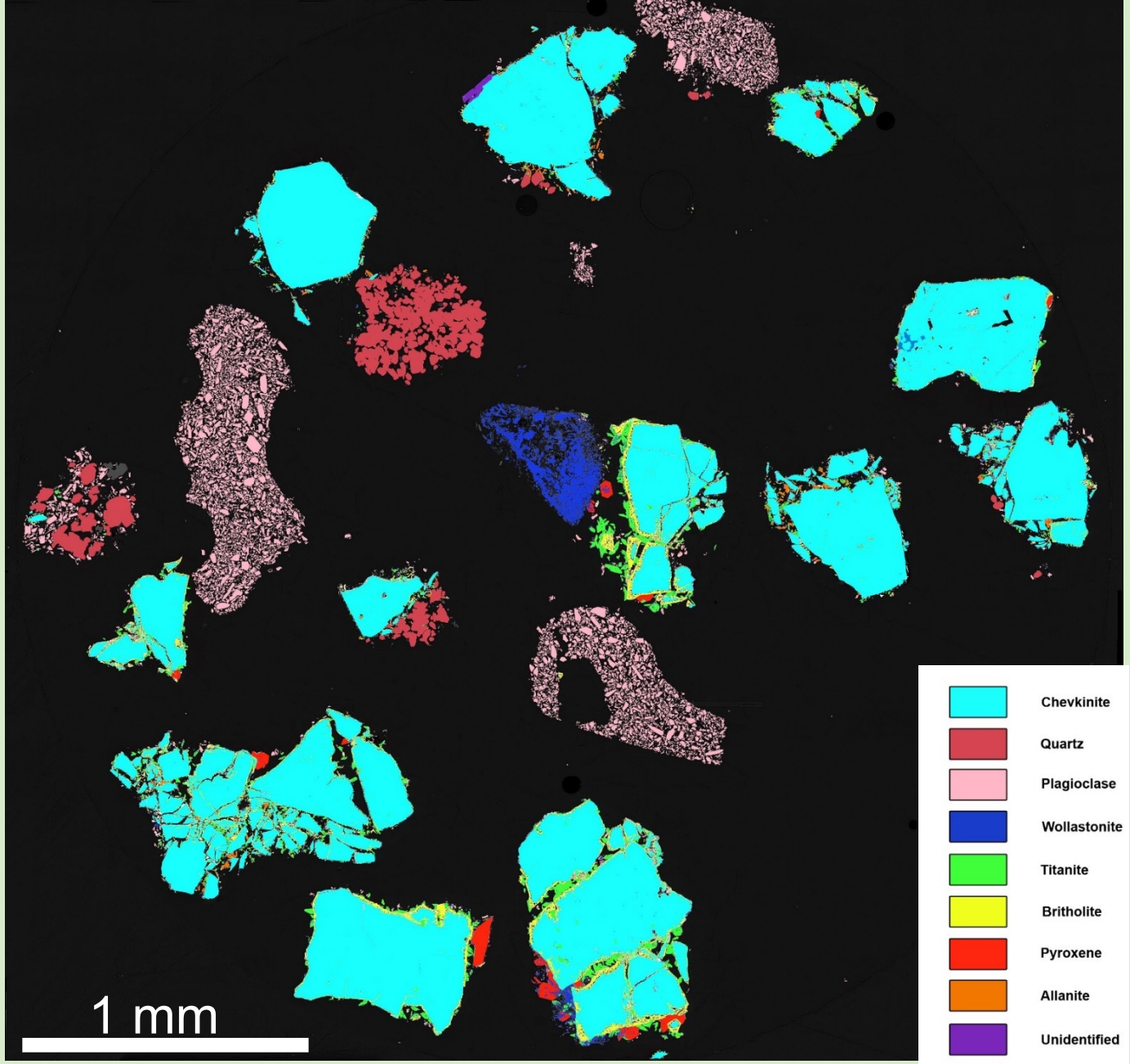

Mineral phases shown in artificial colours on the basis of the EDX hyperscan results

Chevkinite-(Ce) + $Ca(OH)_2$ + Quartz + Albite + H_2O →

Britholite-(Ce) + **Titanite** + Pyroxene (Hedenbergite) + Wollastonite + Allanite-(Ce)

Mineral phases resulted from the experiment **BRITHOLITE-(Ce)**

Different degree of alteration depending of chevkinite crystal size

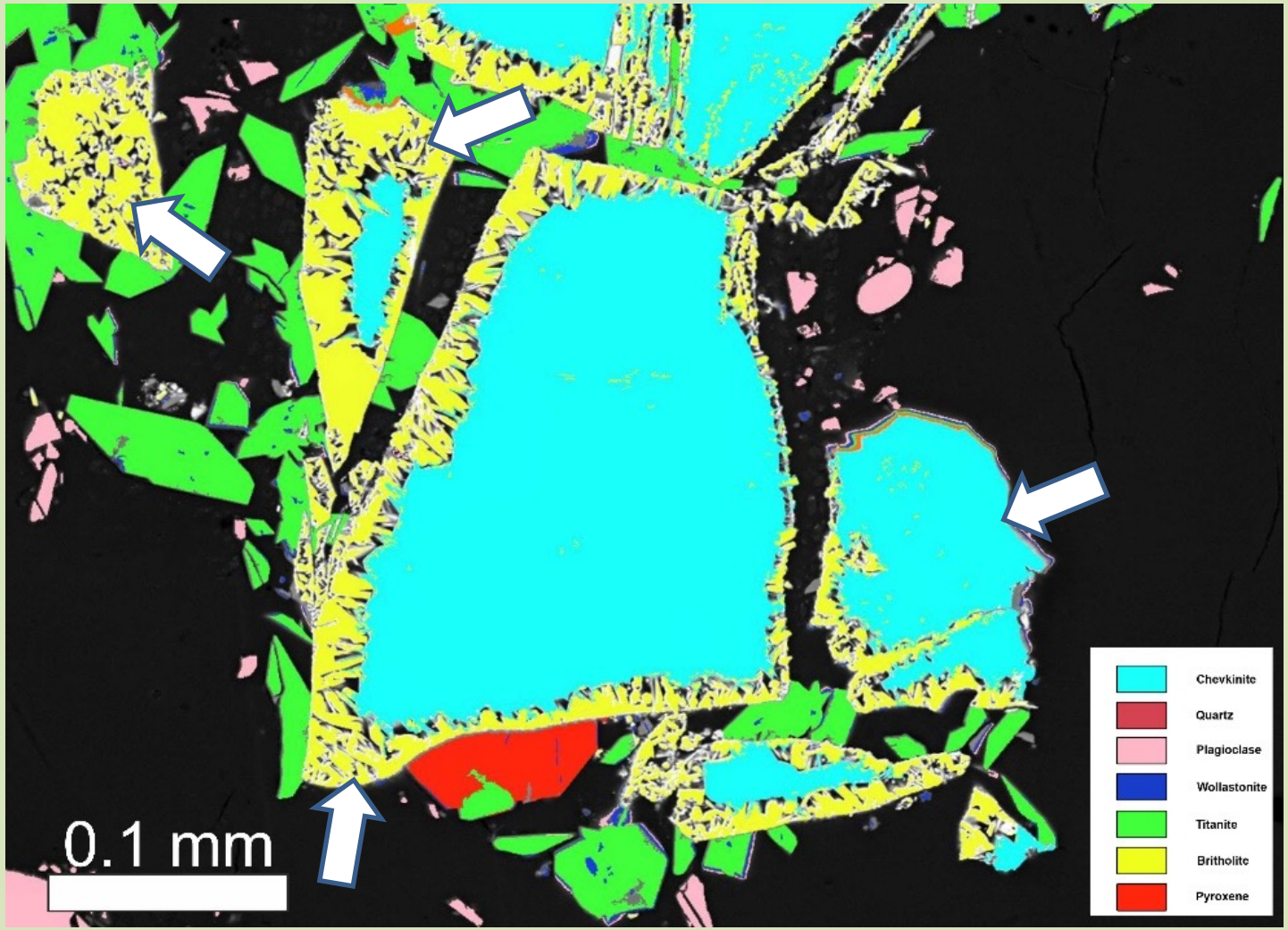

	Chv	Brt
P_2O_5	0.05	0.04
Nb_2O_5	0.46	b.d.
Ta_2O_5	0.13	0.15
SiO_2	18.9	21.38
TiO_2	17.01	0.18
ThO_2	2.09	3.37
Al_2O_3	0.21	b.d.
Y_2O_3	0.08	0.07
La_2O_3	11.4	14.47
Ce_2O_3	22.91	32.27
Pr_2O_3	2.54	3.43
Nd_2O_3	7.98	10.71
Sm_2O_3	0.58	0.88
Gd_2O_3	0.20	0.53
MgO	0.35	b.d.
CaO	2.24	11.31
MnO	0.66	0.06
FeO*	11.82	b.d.
SrO	0.22	0.10
Na_2O	b.d.	0.12
BaO	0.13	0.03
Total	99.96	99.10

Note characteristic, for coupled dissolution and precipitation process (similar to the examples presented by Ruiz-Agudo et al. (2014), position of britholite crystals (it outlines the original shape of the chevkinite crystals)

Mineral phases resulted from the experiment **BRITHOLITE-(Ce)**

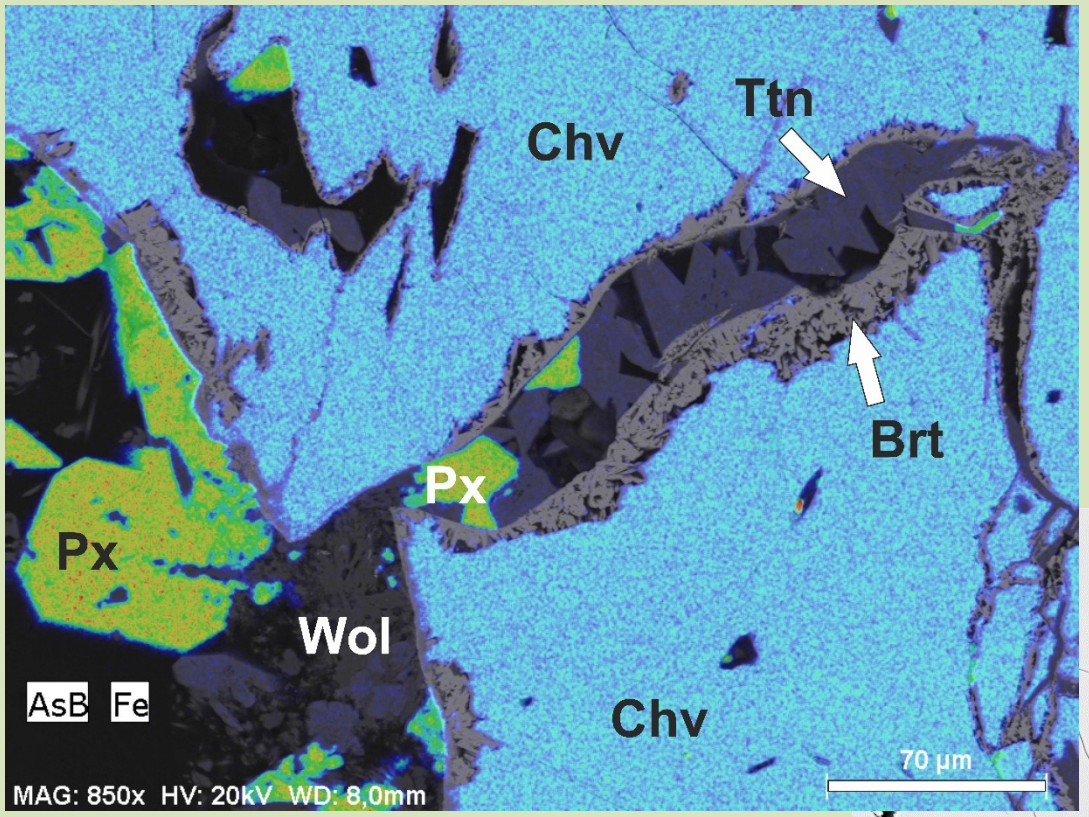

It grow within the cracks being the first crystallizing phase

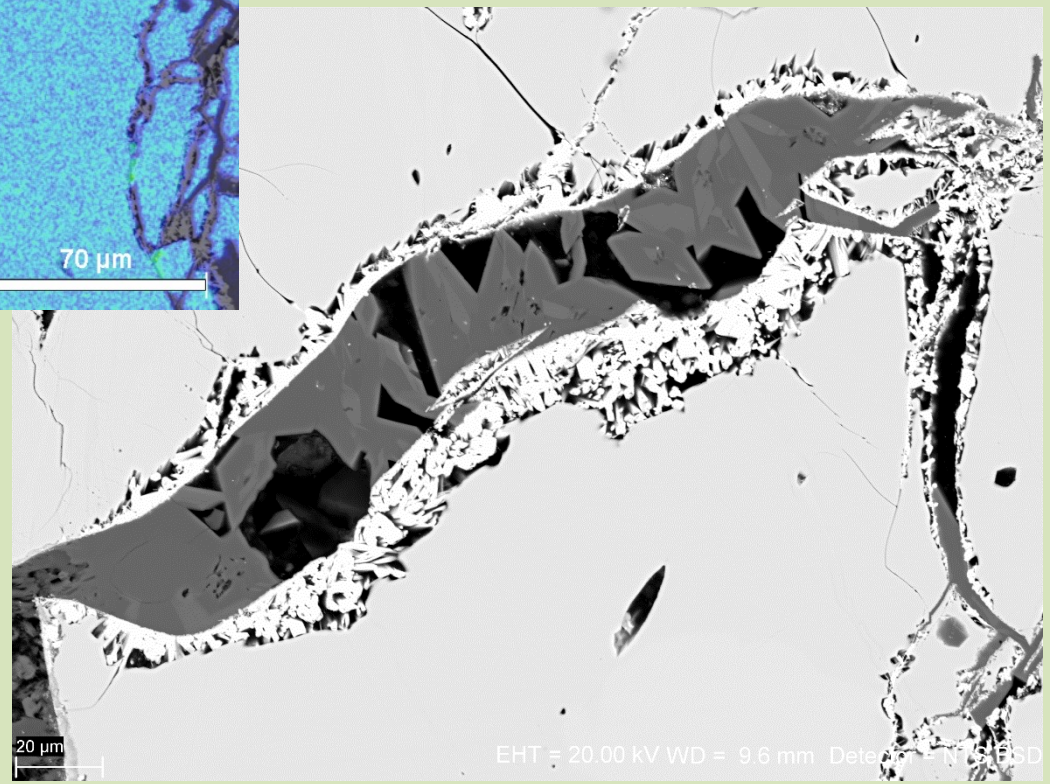

Mineral phases resulted from the experiment **BRITHOLITE-(Ce)**

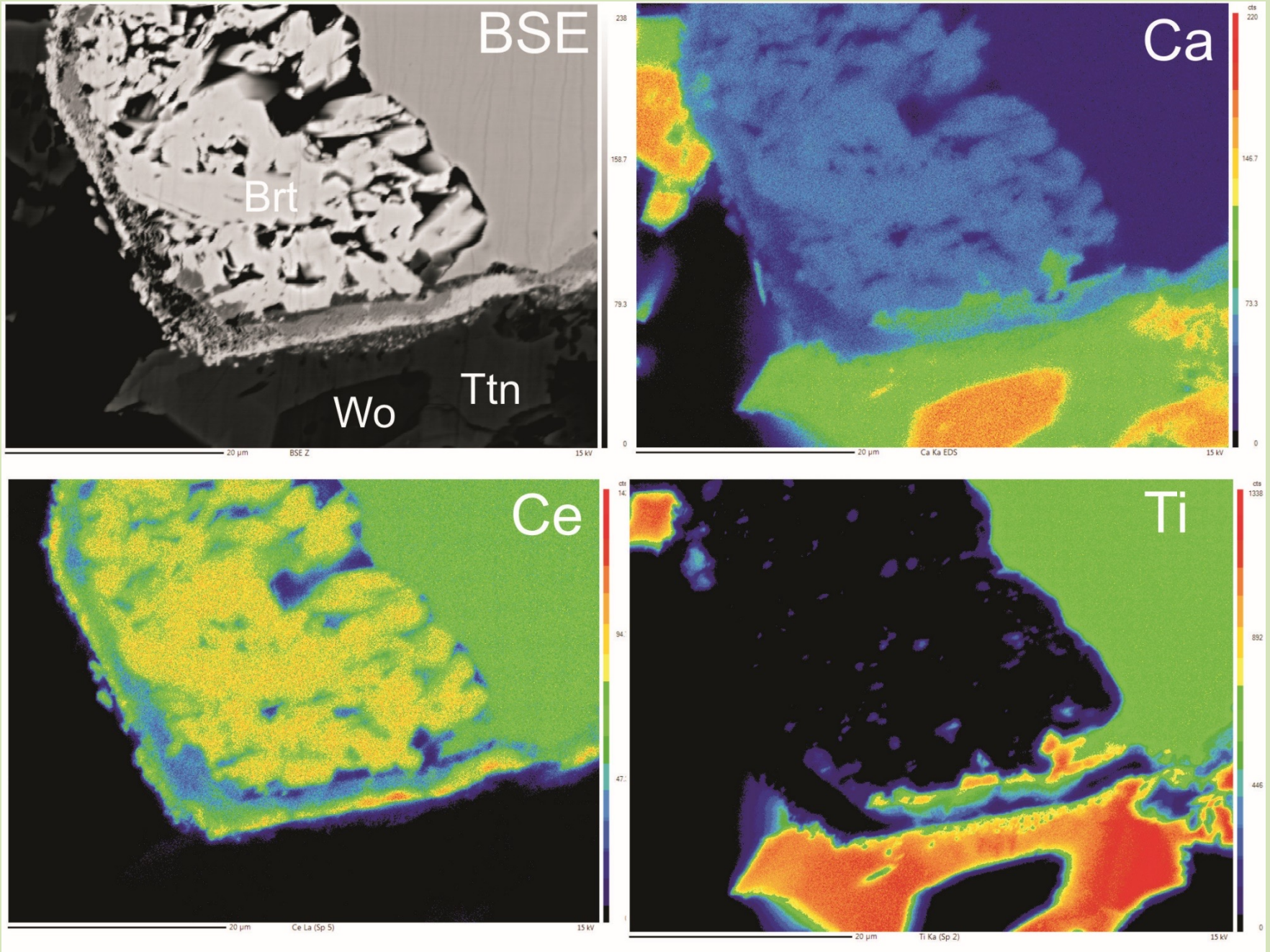

Note considerable porosity in altered britholite zone

Mineral phases resulted from the experiment **TITANITE**

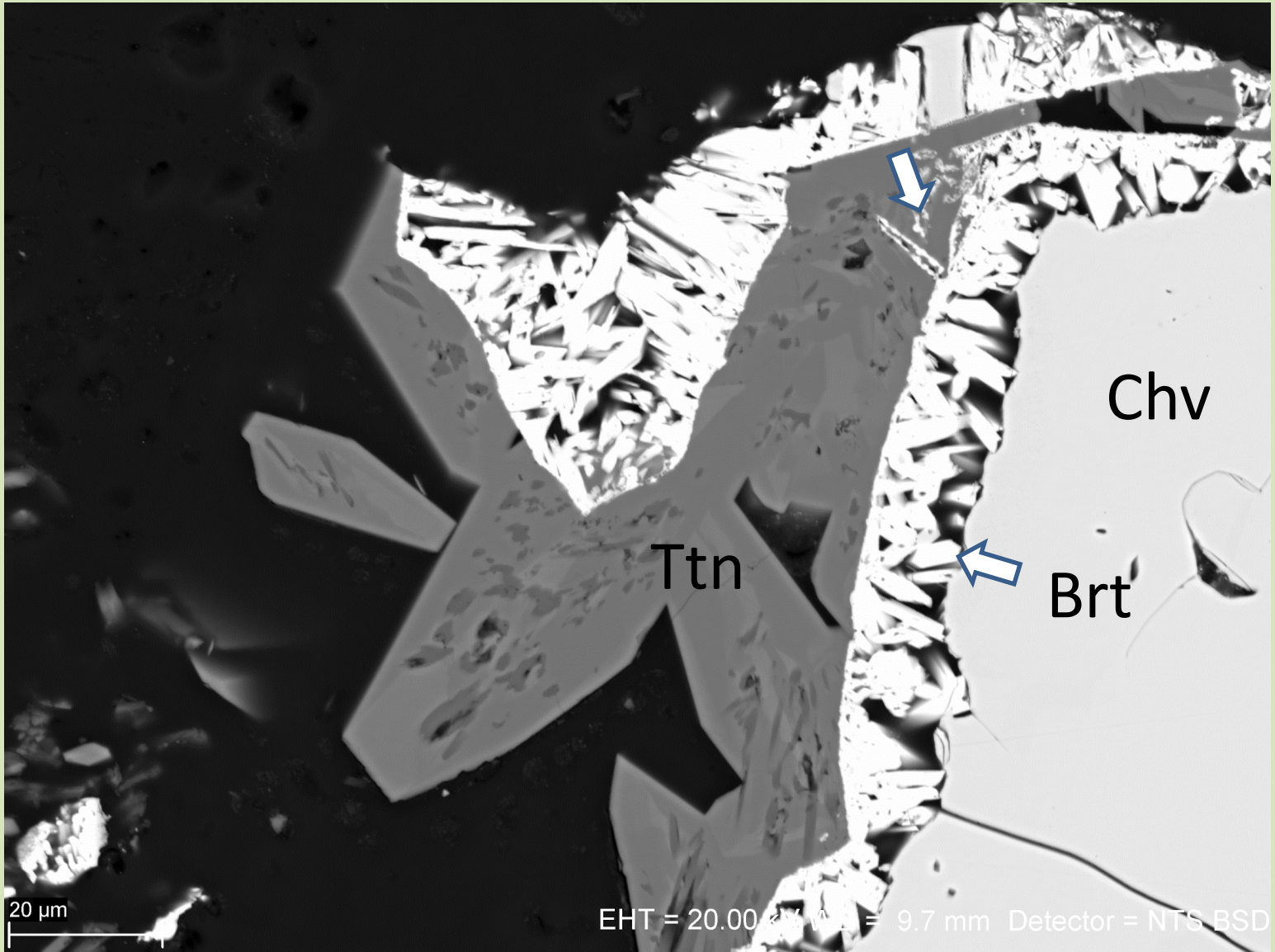

It grows from the reaction front forming **subhedral crystals**

Mineral phases resulted from the experiment **TITANITE**

penetrates up cracks to form veinlets of uncertain structure

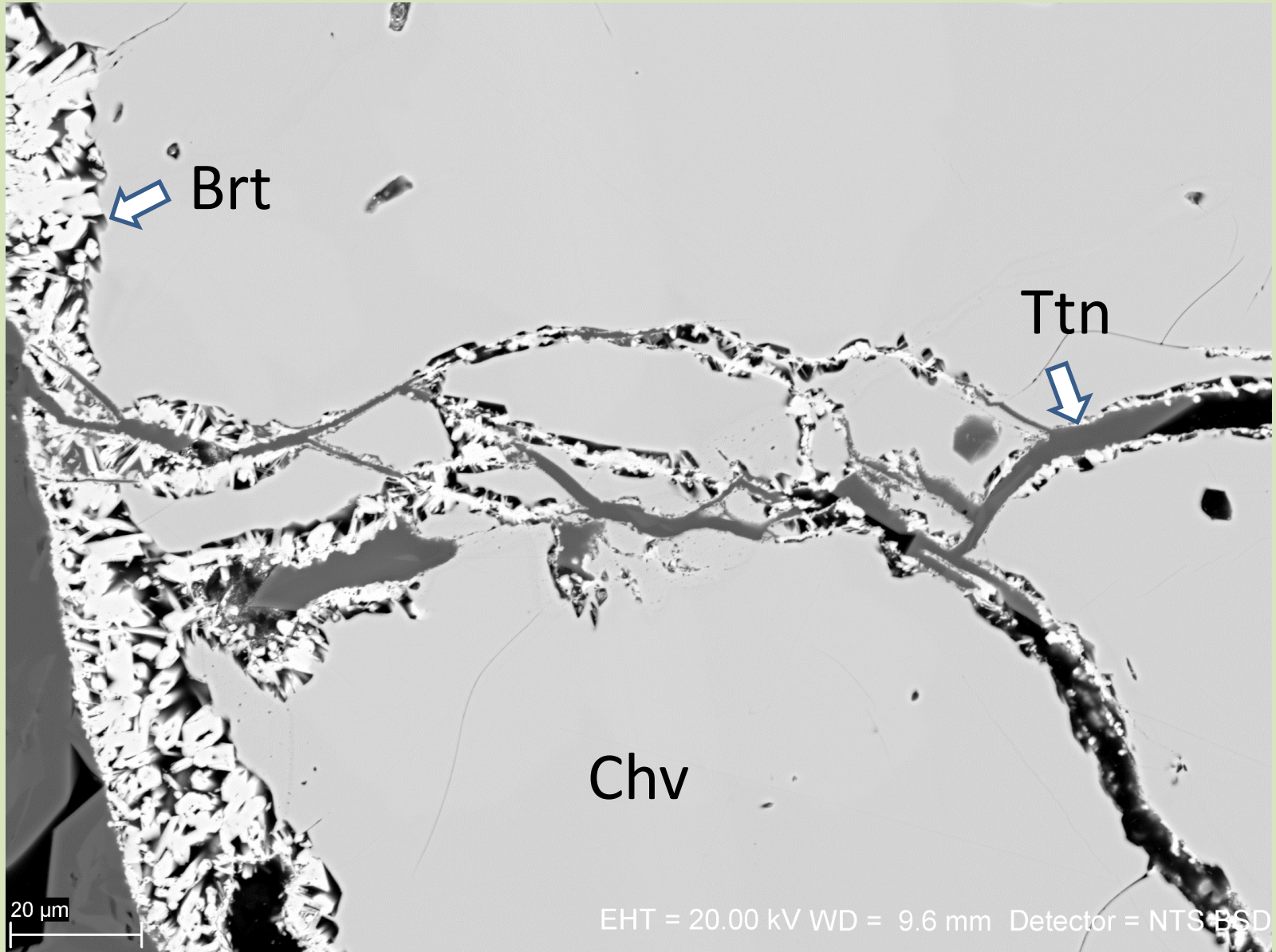

Mineral phases resulted from the experiment **PYROXENE**

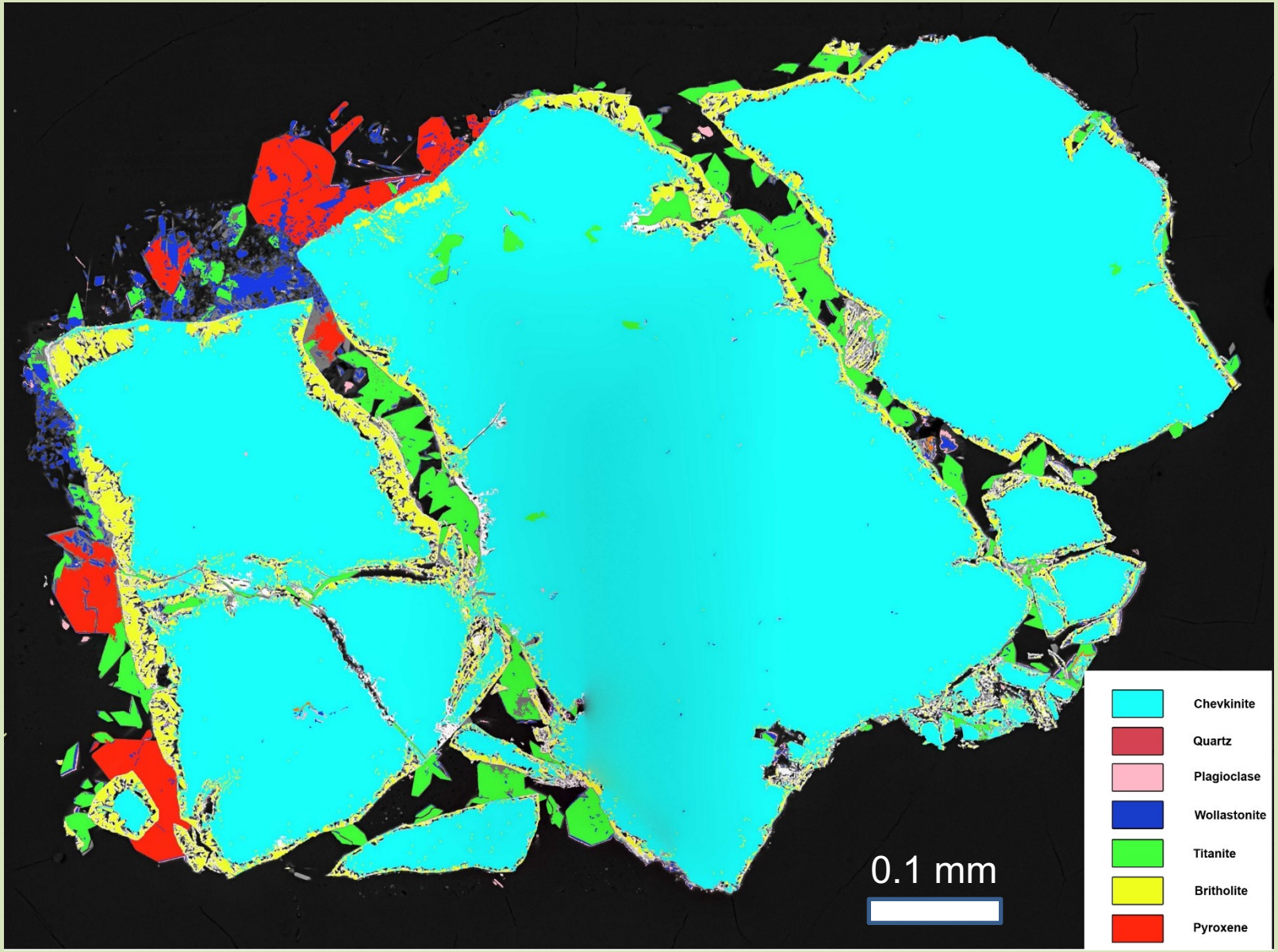

Position of pyroxene growth is similar to that of titanite

Mineral phases resulted from the experiment **WOLLASTONITE**

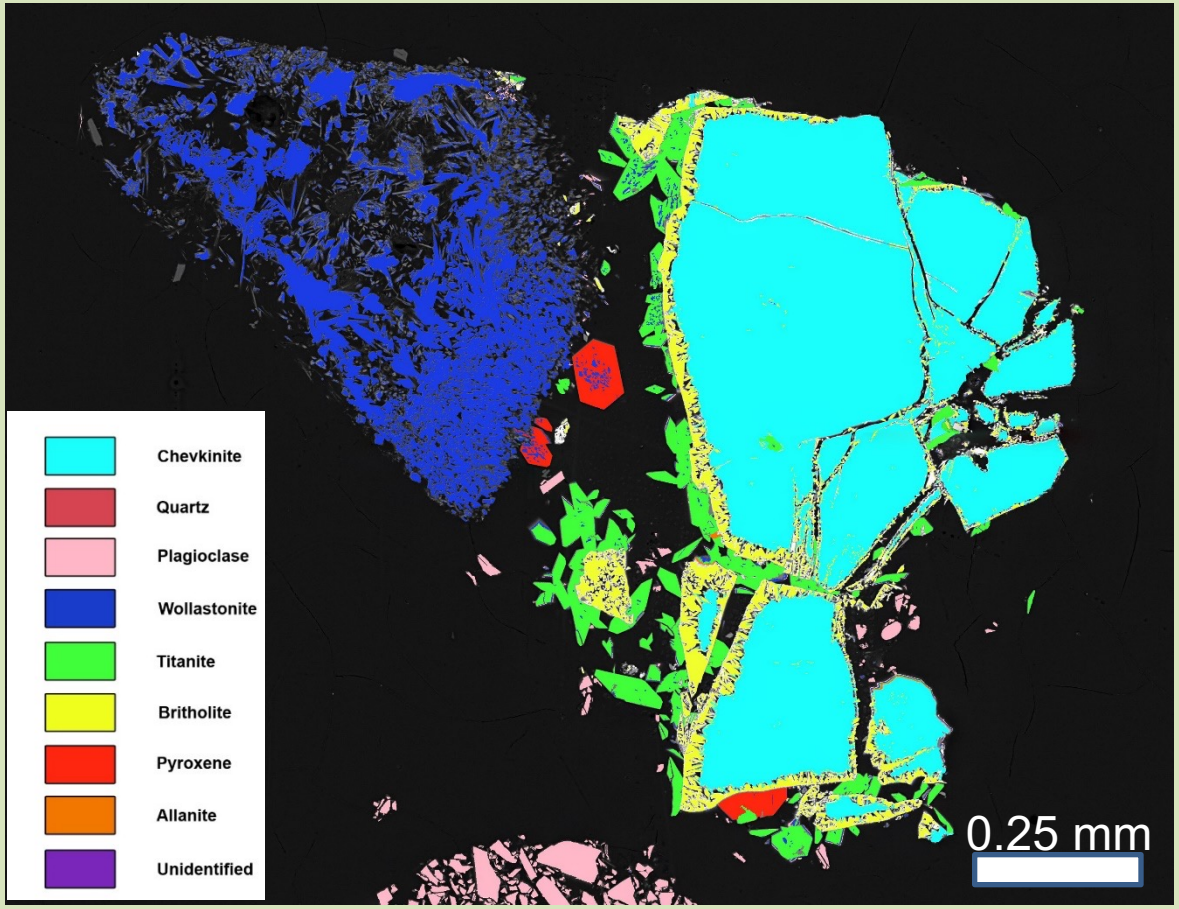

Wollastonite is unusual in natural occurrances of chevkinite hydrothermal alterations but in the experiment it may reflect excess of Ca in the fluid after formation of titanite and pyroxene.

Mineral phases resulted from the experiment **ALLANITE-(Ce)**

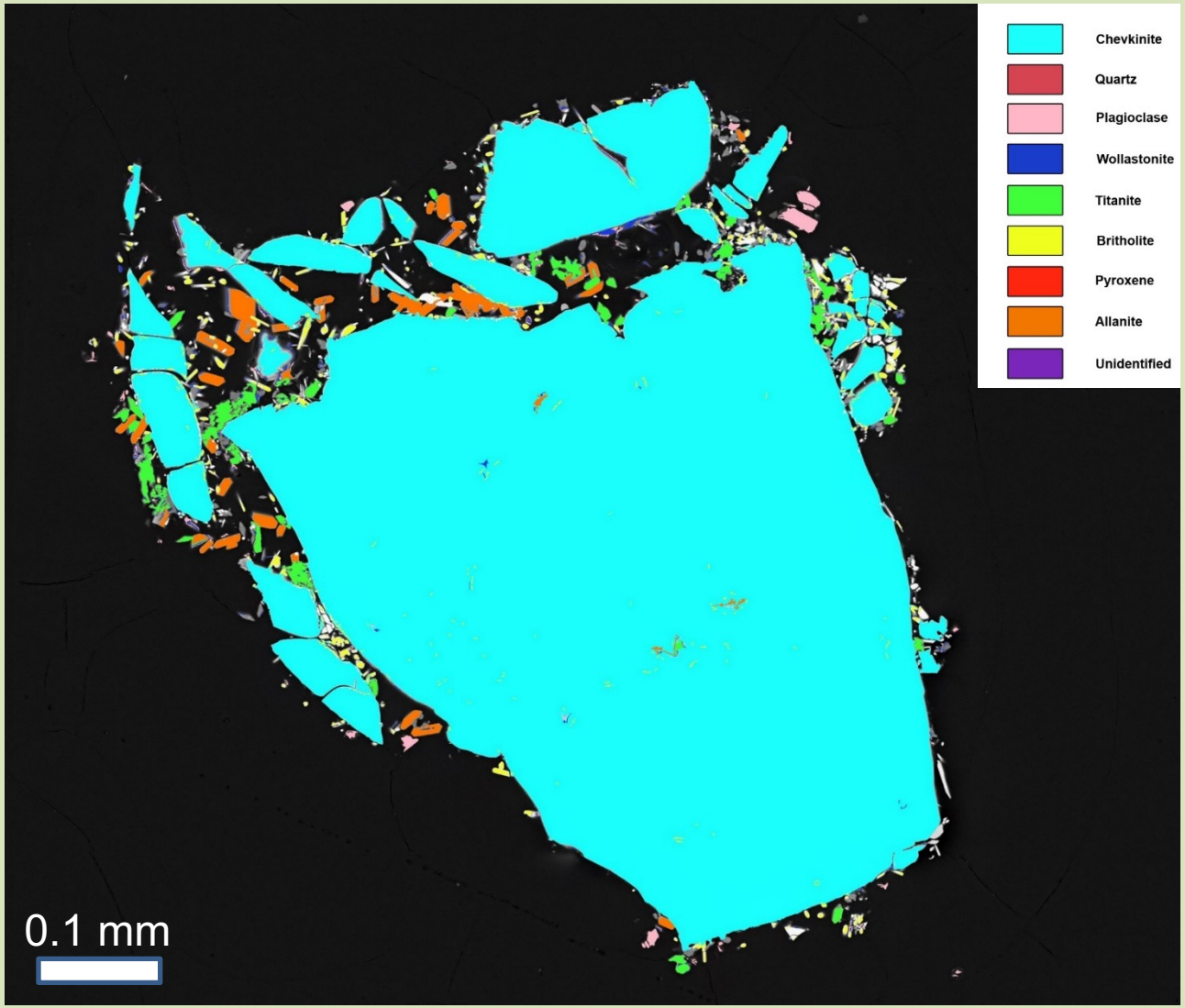

Allanite is rare and its formation may indicate that there were disequilibrium conditions in the capsule. Allanite may be formed in areas where Ca activity was unusually high (see Budzyń et al., 2017)

DISSCUSSION

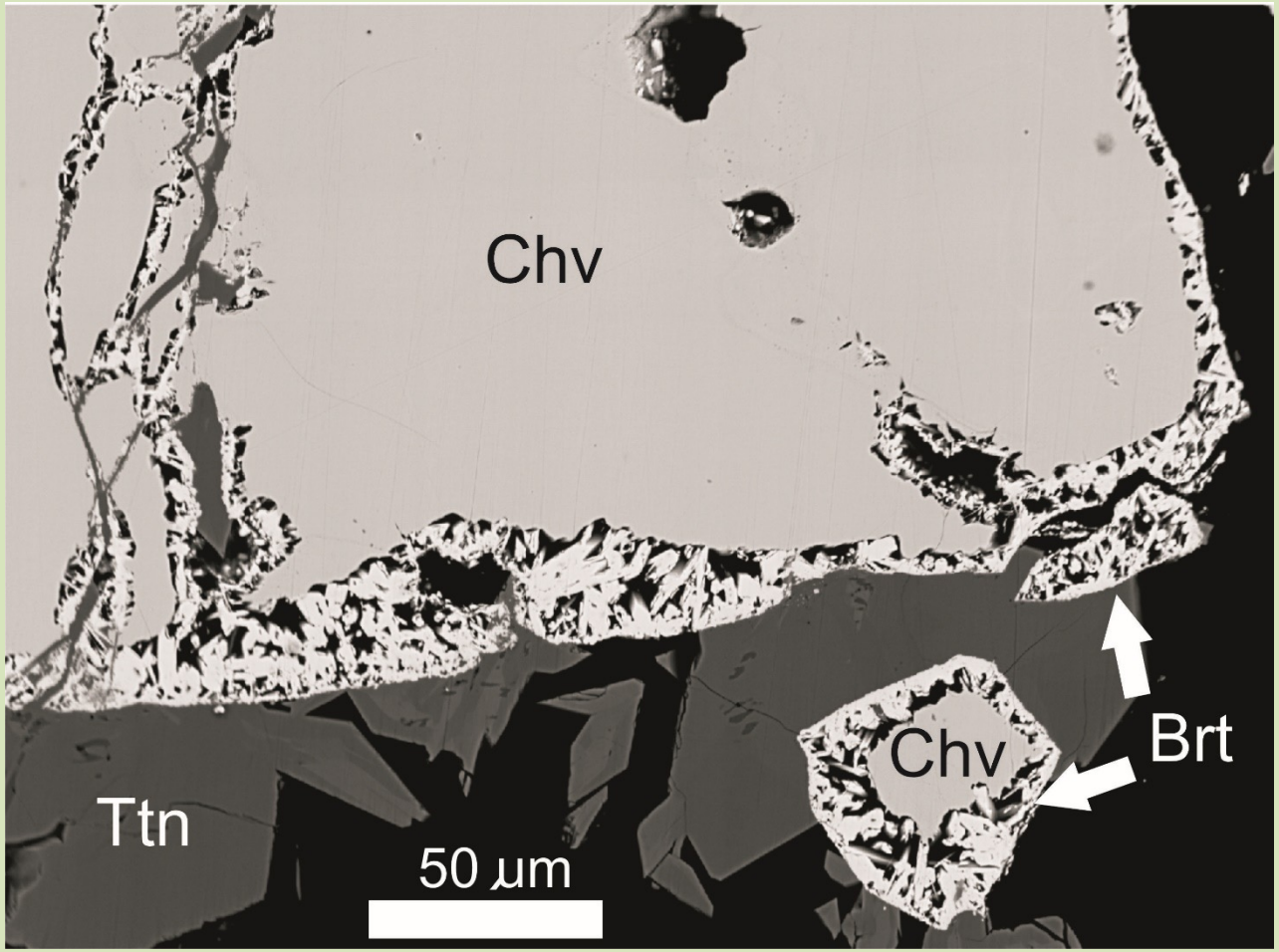

Why are reaction effects different from crystal to crystal?

It depends on the size of the crystals.

DISSCUSSION

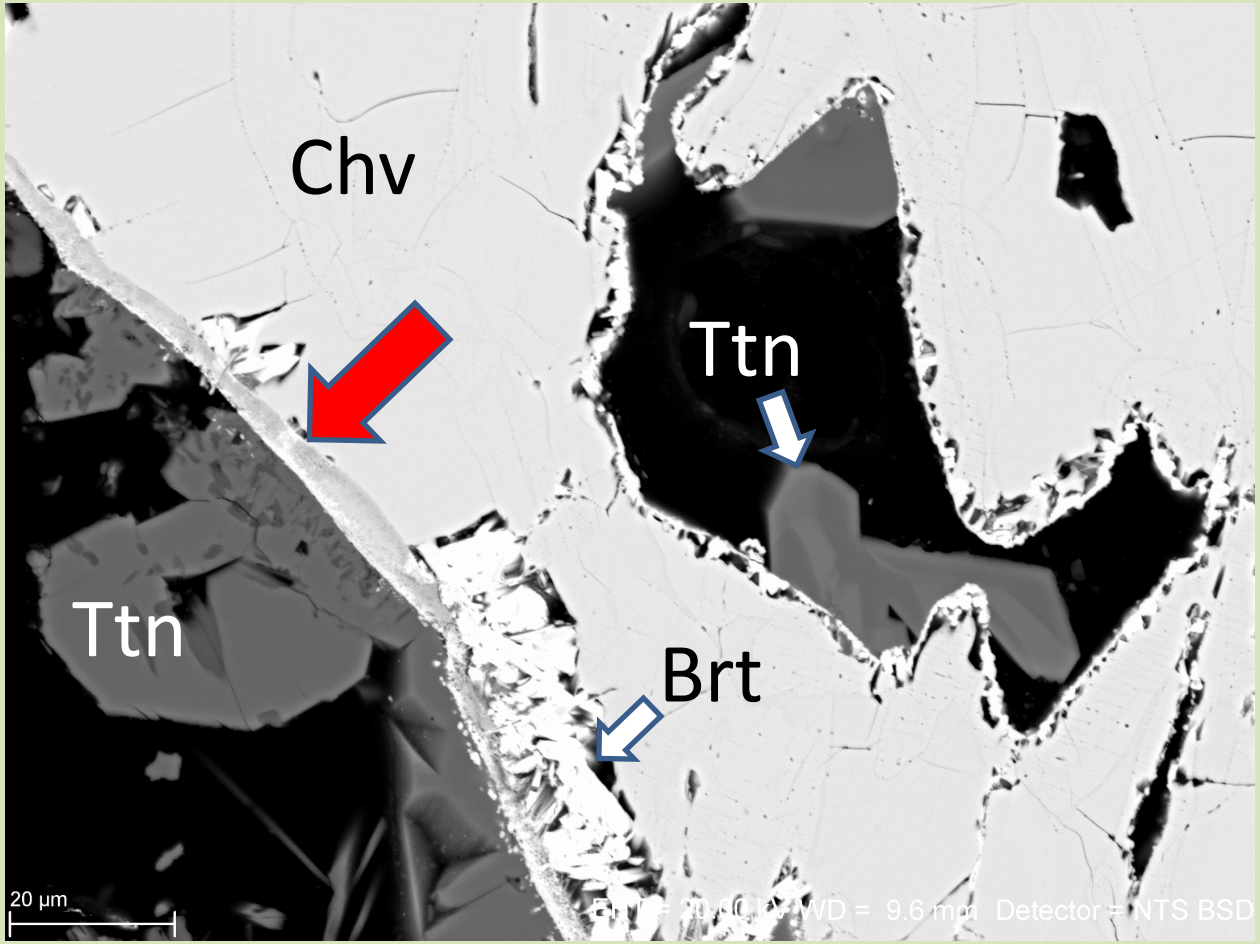

Why are reaction effects different from crystal to crystal?

Starting material had $ThO_2$and UO2 contents ranging from 0.5-2.8 wt.% and 0.05-0.15 wt.% respectively. This may have made certain areas on the rim more prone to reaction than others

DISSCUSSION

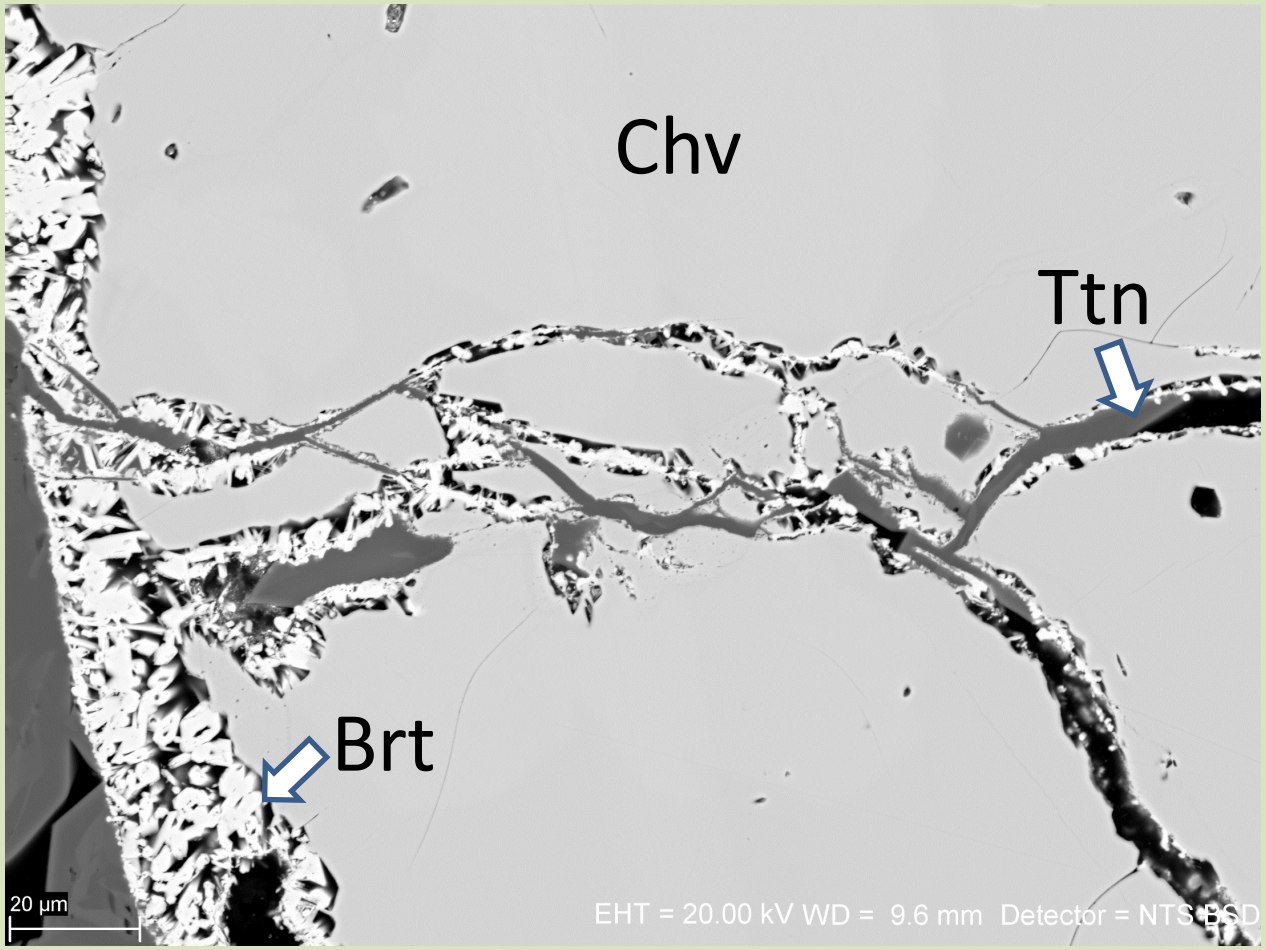

Why are reaction effects different from crystal to crystal?

Cracks and pores are the corridors for fluids and created during the coupled dissolution and precipitation process additional porosity let the fluids penetrate deeper into the chevkinite crystals

DISSCUSSION

Partitioning of elements between phases

REE elements

Rather small amounts of the REE (up to 6 wt.% or 0.07 apfu) have entered titanite.

Similarly, the content of REE in pyroxene is low (below 1 wt.% or 0.02 apfu)

The REE mostly partitioned into britholite and chondrite normalised plots for the chevkinite-(Ce) and britholite-(Ce) are very similar, what indicates that the LREE were not significantly fractionated during alteration, although concentrations of the REE oxides are higher in britholite (up to 62 % REE_2O_3)

Allanite-(Ce) has variable REE content, up to 24% REE_2O_3 and shows more distinct LREE fractionation

Th and U

Th and U are incorporated only into britholite-(Ce) structure where Th has higher concentrations (up to 4 wt%) than in chevkinite-(Ce) (up to 2.8 wt%)

CONCLUSIONS

- Chevkinite-(Ce) was readily altered at 600 ^{o}C and 400 MPa by a fluid containing $Ca(OH)_2$. The main products were britholite-(Ce) and titanite with some amounts of hedenbergite what contrasts with results observed in natural environments of hydrothermal alterations (Bagiński et al. 2015, 2016, Macdonald et al. 2017,2019) where the main result were allanite and titanite
- Alteration occurred on both the rims and along cracks. The main alteration mechanism was dissolution-reprecepitation (concerns mainly britholite-(Ce))
- Where britholite-(Ce) formed, it incorporated the REE from the chevkinite-(Ce) without significantly fractionating them. Rare allanite-(Ce) on the other hand, also incorporated the REE but with higher La/Sm ratios than the original.

Acknowledgements. Study was financed from the National Science Centre, Poland; grant no. 2017/26/M/ ST10/00407.

REFERENCES

- Bagiński B, Macdonald R, Dzierżanowski P, Zozulya D, Kartashov PM (2015) Hydrothermal alteration of chevkinite-group minerals. Part 1. Hydration of chevkinite-(Ce). Mineral Mag 79: 1019-1037
- Bagiński B, Zozulya D, Macdonald R, Kartashov PM, Dzierżanowski P (2016) Low-temperature hydrothermal alteration of a rare-metal rich quartz-epidote metasomatite from the El'ozero deposit, Kola Peninsula, Russia. Eur J Mineral 28: 789-810
- Budzyń B, Harlov DE, Williams ML, Jercinovic MJ (2011) Experimental determination of stability relations between monazite, fluorapatite, allanite, and REE-epidote as a function of pressure, temperature, and fluid composition. Am Mineral 96: 1547-1567
- Budzyń B, Harlov DE, Kozub-Budzyń GA, Majka J (2017) Experimental constraints on the relative stabilities of the two systems monazite-(Ce) – allanite-(Ce) – fluorapatite and xenotime-(Y) – (Y,HREE)-rich epidote – (Y,HREE)-rich fluorapatite, in high Ca and Na-Ca environments under P-T conditions of 200-1000 MPa and 450-750 °C. Mineral Petrol 111: 183-217
- Macdonald R, Bagiński B, Zozulya D (2017) Differing responses of zircon, chevkinite-(Ce), monazite-(Ce) and fergusonite-(Y) in hydrothermal alteration: Evidence from the Keivy alkaline province, Kola Peninsula, Russia. Mineral Petrol 111: 523-545
- Macdonald R, Bagiński B, Belkin HE, Stachowicz M (2019) Composition, paragenesis and alteration of the chevkinite group of minerals. Am Mineral 104*:* 349-367
- Putnis A (2009) Mineral replacement reactions. Rev Mineral Geochem 70: 87-124
- Ruiz-Agudo E, Putnis CV, Putnis A (2014) Chem Geol 383: 132-146


Thank you very much for your attention